Applied Catalysis A: General 394 (2011) 124–131

Contents lists available at ScienceDirect

Applied Catalysis A: General

journal homepage: www.elsevier.com/locate/apcata

Ni catalysts supported over $MgAl_2O_4$ modified with Pr for hydrogen production from ethanol steam reforming

M. Noelia Barroso, Agustín E. Galetti, M. Cristina Abello*

INTEQUI, Instituto de Investigaciones en Tecnología Química - (UNSL-CONICET). Chacabuco y Pedernera, Casilla De Correo 290, (5700) San Luis, Argentina

ARTICLE INFO

Article history:
Received 15 October 2010
Received in revised form
21 December 2010
Accepted 23 December 2010
Available online 4 January 2011

Keywords:
$Ni/MgAl_2O_4$ catalysts
Hydrogen
Ethanol steam reforming
Carbon deposits

ABSTRACT

$MgAl_2O_4$ spinel oxide-supported Ni catalysts modified with Pr have been prepared by wet impregnation method with 8 wt.% Ni and variable loadings of Pr (0–7 wt.%). The samples were characterized by ICP, BET, XRD, TPR, SEM, Raman and TG-TPO and they were tested in ethanol steam reforming reaction.

The XRD of the samples revealed the presence of spinel phase $MgAl_2O_4$, NiO and weak lines of PrO_2/Pr_6O_{11}. The addition of Pr slowed down the deactivation rate affecting the amount and the type of carbon deposit. Under reactive conditions, the system with 2.6 Pr wt.% showed the best performance and although it presented filamentous carbon, this catalytic system kept around 80% ethanol conversion during the reaction time (40 h) under severe reforming conditions without reactor plugging.

1. Introduction

The growing of the world population and the changes in the society behavior have produced a vertiginous increase in the energetic demand. The decrease in fossil resources and mainly the necessity to protect the environment have led to the urgent search for alternative energetic sources [1,2]. An interesting option is the hydrogen production from ethanol steam reforming. Ethanol has several advantages compared with other raw materials but the most important one is its renewable origin [3,4]. It can be obtained from biomass fermentation (e.g. corn, sugar cane, and cellulose) and it slightly contributes to green house effect since CO_2 is recycled through photosynthesis during the plant growth. Besides, it has relatively high hydrogen content and its reaction with water under steam-reforming conditions is able to produce 6 mol of H_2 per mole of reacted ethanol:

$$CH_3CH_2OH + 3H_2O \rightarrow 6H_2 + 2CO_2$$

Different catalytic systems have been studied for this reaction including noble metals [5–8], nickel [9–11], nickel–copper [12,13], cobalt [14–22], etc. supported over several supports. Ni catalysts have been used in commercial scale in several reforming processes for more than 40 years [23], especially for their high activity to break C–C bond and their low cost compared with noble metals. The main disadvantages of Ni catalysts are related to deactivation by coke formation, sintering and inactive phase transformation. There are many studies about the carbon formation on Ni systems [24–27] and a lot of effort has been focused on developing new Ni stable catalysts with improved resistance to coke formation. In a previous work the addition of Ce to $Ni/ZnAl_2O_4$ catalyst was examined and an important decrease in carbon deposition was observed in ethanol steam reforming reaction [28]. These improvements have been attributed to a better Ni^{2+} dispersion over the modified catalyst and to the high oxygen mobility from ceria or from Ni–Ce boundary which allowed a higher residual activity and an improved coking resistance.

Praseodymium and cerium are adjacent in the periodic table and their oxides have many similar characteristics [29]. Praseodymium has a special position within the rare-earth elements since it can form a homologous series of oxides with variable valence states (+3 and +4) and a large number of stoichiometrically defined oxides: Pr_nO_{2n-2}, with $n = 4, 7, 9, 10, 11, 12, \infty$ [30] being the extreme cases Pr_2O_3 and PrO_2. As ceria these oxides have high oxygen ion mobility and therefore the ability to acquire or release oxygen meanwhile they convert their oxidation states between +3 and +4. However, differences have been reported on Rh/CeO_2 and Rh/PrO_x catalysts concerning to the relative amount of H_2 that desorbs at low and high temperatures [31]. In studies about interaction with CO, Borchert et al. have also reported that CO is not adsorbed on Pr cations (Pr^{3+} or Pr^{4+}) whereas adsorption occurs on Ce^{4+} at room temperature [32]. Recently, the influence of Pr in dry methane reforming catalysts produced from perovskites has been studied [33]. These authors have reported a high resistance to deactivation

* Corresponding author.
E-mail address: cabello@unsl.edu.ar (M.C. Abello).

0926-860X/$ – see front matter © 2011 Elsevier B.V. All rights reserved.
doi:10.1016/j.apcata.2010.12.038

as a consequence of the redox chemistry of praseodymium oxides. They have suggested that praseodymium oxides have a high facility to reoxidize and could react with CO_2 during the reforming reaction to form PrO_2 and CO. These aspects render very attractive to evaluate the influence of Pr in Ni based catalysts, even though PrO_x oxides are more expensive than CeO_2 (nowadays around 15%). Besides, as far as we know, there has been no report on their use for the steam reforming of ethanol.

Moreover, suitable supports should be resistant to the high temperatures applied in ethanol steam reforming and they should be able to maintain the metal dispersion as high as possible during reaction. Recently, the type spinel oxides (AB_2O_4) have been proposed as catalytic supports due to the low acidity and resistance to coking and sintering [34,35]. Guo et al. have employed $MgAl_2O_4$ as support for dry reforming of methane [36] and they have found a higher activity and better stability over Ni/$MgAl_2O_4$ than on Ni/γ-Al_2O_3. Auprêtre et al. have also obtained an improved deactivation resistance with catalysts prepared over $MgAl_2O_4$ [37]. In a previous work it was also found that $MgAl_2O_4$ was a better support than $ZnAl_2O_4$ [38]. Taking into account this information, the preparation, characterization and catalytic activity of Ni supported over $MgAl_2O_4$ modified by Pr addition in the ethanol steam reforming are discussed in this work.

2. Experimental

2.1. Catalyst preparation

$MgAl_2O_4$ support was prepared by the citrate method. Citric acid was added to an aqueous solution that contained the stoichiometric quantities of $Al(NO_3)_3{\cdot}9H_2O$ and $Mg(NO_3)_2{\cdot}6H_2O$. An equivalent of acid per total equivalent of metals was used. The solution was stirred for 10 min and held at boiling temperature for 30 min. Then the solution was concentrated by evaporation under vacuum in a rotavapor at 75 °C until a viscous liquid was obtained. Finally, dehydration was completed by drying the sample in a vacuum oven at 100 °C for 16 h. The sample was calcined in a 100 mL min^{-1} flow under the following program: at 500 °C in N_2 flow for 2 h, at 700 °C in O_2 (10%)/N_2 flow for 2 h and finally, in air at 700 °C for 2 h to remove the carbonaceous residues from citrate chains. The sample was denoted as MgAl.

Supported Ni catalysts were prepared by wet impregnation using an aqueous solution of $Ni(CH_3COO)_2{\cdot}4H_2O$ (Aldrich, 98%). The nominal composition of Ni was 8 wt.%. After impregnation, the solid was dried at 100 °C overnight. Then, different Pr amounts from an aqueous solution of $Pr(CH_3COO)_3{\cdot}xH_2O$ (Aldrich, 99.9%) were incorporated by wet impregnation. The Pr nominal loading varied from 0 to 10 wt.%. The samples were dried at 100 °C for 16 h and finally, they were calcined in air at 600 °C for 3 h. The catalysts were denoted as Ni/Pr_x/MgAl x being an indicative number of nominal Pr loading. Thus, Ni/Pr_5/MgAl indicates a catalyst with 5 wt.% of nominal Pr.

2.2. Catalyst characterization

All samples were characterized using different physicochemical methods.

2.2.1. Chemical composition

Praseodymium chemical composition was performed by inductively coupled plasma-atomic emission spectroscopy (ICP) by using a sequential ICP spectrometer Baird ICP 2070 (Bedford, USA) with a Czerny Turner monochromator (1 m optical path). Alkali fusion with $KHSO_4$ and a subsequent dissolution with HCl solution brought the samples into solution.

2.2.2. BET surface area

BET surface areas were measured by using a Micromeritics Gemini V analyzer by adsorption of nitrogen at −196 °C on 200 mg of sample previously degassed at 240 °C for 16 h under flowing N_2.

2.2.3. X-ray diffraction (XRD)

XR diffraction patterns were obtained with a RIGAKU diffractometer operated at 30 kV and 20 mA by using Ni-filtered CuKα radiation (λ = 0.15418 nm) at a rate of 3° min^{-1} from 2θ = 20° to 80°. The powdered samples were analyzed without a previous treatment after deposition on a quartz sample holder. The identification of crystalline phases was made by matching with the JCPDS files.

2.2.4. Thermal gravimetry (TG)

The analyses were recorded by using TGA 51 Shimadzu equipment. The samples, c.a. 15 mg, were placed in a Pt cell and heated from room temperature to 1000 °C at a heating rate of 10 °C min^{-1} with a gas feed (air) of 50 mL min^{-1}.

2.2.5. Temperature programmed reduction (TPR)

Studies were performed in a conventional TPR equipment. This apparatus consists of a gas handling system with mass flow controllers (Matheson), a tubular reactor, a linear temperature programmer (Omega, model CN 2010), a PC for data retrieval, a furnace and various cold traps. Before each run, the samples were oxidized in a 50 mL min^{-1} flow of 20 vol.% O_2 in He at 300 °C for 30 min. After that, helium was admitted to remove oxygen and finally, the system was cooled to 25 °C. The samples were subsequently contacted with a 50 mL min^{-1} flow of 5 vol.% H_2 in N_2, heated at a rate of 5 °C min^{-1}, from 25 °C to a final temperature of 700 °C and held at 700 °C for 1 h. Hydrogen consumption was monitored by a thermal conductivity detector after removing the formed water. The characteristic number P proposed by Malet and Caballero [39] defined as $\beta S_o/(V^* C_o)$, where S_o is the initial amount of reducible species in the sample (μmol), V^* is the total flow rate (mL min^{-1}), C_o is the initial hydrogen concentration in the feed (μmol H_2 mL^{-1}) and β is the heating rate (°C min^{-1}), was ≈10 °C in order to obtain an unperturbed reduction profile. The peak areas were calibrated with H_2(5 vol.%)/N_2 mixture injections.

2.2.6. Raman spectroscopy

The Raman spectra were recorded using a Lab Ram spectrometer (Jobin-Yvon) coupled to an Olympus confocal microscope equipped with a CCD with the detector cooled to about −70 °C using the Peltier effect. 100× objective lens were used for simultaneous illumination and collection. The excitation wavelength was in all the cases 532 nm (Spectra Physics argon-ion laser). The laser power was set at 30 mW. Integration times ranged from a few seconds to a few minutes depending on the sample. A scanning range between 100 and 2000 cm^{-1} was applied.

2.2.7. Scanning electron microscopy and energy dispersive X-ray spectroscopy (SEM–EDX)

Scanning electron micrographs were obtained in a LEO 1450 VP. This instrument equipped with an energy dispersive X-ray microanalyzer (EDAX Genesis 2000) and a Si(Li) detector allowed the analytical electron microscopy measurements. The samples were sputter coated with gold.

2.3. Catalytic test

The ethanol steam reforming reaction was carried out in a stainless steel tube with an internal diameter of 4 mm operated at atmospheric pressure. The reactor was placed in a vertical furnace which was controlled by a programmable temperature controller.

Table 1
Characteristics of $Ni/Pr_x/MgAl_2O_4$ catalysts.

Catalyst	Pr wt.%[a]	S_{BET}, m^2/g
MgAl	–	170
$Ni/Pr_0/MgAl$	0	138
$Ni/Pr_1/MgAl$	0.6 (1)	144
$Ni/Pr_3/MgAl$	1.8 (3)	110
$Ni/Pr_5/MgAl$	2.6 (5)	133
$Ni/Pr_{10}/MgAl$	6.7 (10)	109

[a] Determined by ICP. Parenthesis values correspond to nominal ones.

The reaction temperature was measured with a coaxial K thermocouple. The feed to the reactor was a gas mixture of ethanol, water and helium (99.999% research grade purified by a MnO_2-celite oxytrap). Ethanol–water was fed to an evaporator (operated at 130 °C) through an isocratic pump operated at 0.15 mL min^{-1}. The flow rates of gas stream were controlled by mass flowmeters. The experimental set-up was supplied with a low pressure proportional relief valve for early detection of the plugged catalytic bed. The molar ratio in the feed was H_2O:C_2H_5OH = 4.9:1 being the ethanol flow 1.02×10^{-3} mol min^{-1}. The catalyst weight was 50 mg (0.3–0.4 mm particle size range) diluted in quartz (inert:catalyst ratio = 5.5). The catalyst was heated to reaction temperature under He flow, then the mixture with $C_2H_5OH + H_2O$ was allowed to enter into the reactor to carry out the catalytic test. Fresh samples were used in all the experiment runs. The reactants and reaction products were analyzed on-line by gas chromatography. H_2, CH_4, CO_2 and H_2O were separated by a 1.8 m Carbosphere (80–100 mesh) column and analyzed by TC detector. Nitrogen was used as an internal standard. Besides, CO was analyzed by a flame ionization detector after passing through a methanizer. Higher hydrocarbons and oxygenated products (C_2H_4O, C_2H_4, C_3H_6O, C_2H_5OH, etc.) were separated in Rt-U PLOT capillary column and analyzed with FID using N_2 as carrier gas. The homogeneous contribution was tested with the empty reactor. These runs showed an ethanol conversion lower than 1% at 650 °C.

Ethanol conversion, selectivity to carbon products and hydrogen yield were defined as

$$X_{EtOH} = \frac{F_{EtOH}^{in} - F_{EtOH}^{out}}{F_{EtOH}^{in}} 100$$

$$S_i = \frac{\nu_i F_i^{out}}{2(F_{EtOH}^{in} - F_{EtOH}^{out})} 100$$

$$Y_{H_2} = \frac{F_{H_2}^{out}}{F_{EtOH}^{in}}$$

F_i^{in} and F_i^{out} are the molar flow rates of product "i" at the inlet and outlet of the reactor, respectively, and ν_i is the number of carbon atoms in "i".

3. Results and discussion

In Table 1, the BET specific surface areas for support and samples are shown. In spite of the thermal treatment, at 600 °C for 3 h, high values were obtained. The nickel impregnation decreased in about 20% the specific surface area whereas the Pr addition did not substantially decrease them. Guo et al. [40] have prepared a support based on magnesium aluminate by sol–gel method and they have reported specific surface areas between 170 and 200 m^2/g. These authors [36] have also developed Ni catalysts using $MgAl_2O_4$ spinel prepared from co-precipitation method. These catalysts showed a significant decrease in specific surface areas (80 and 78 m^2/g, respectively) after impregnation with 5 and 10 Ni wt.%. The

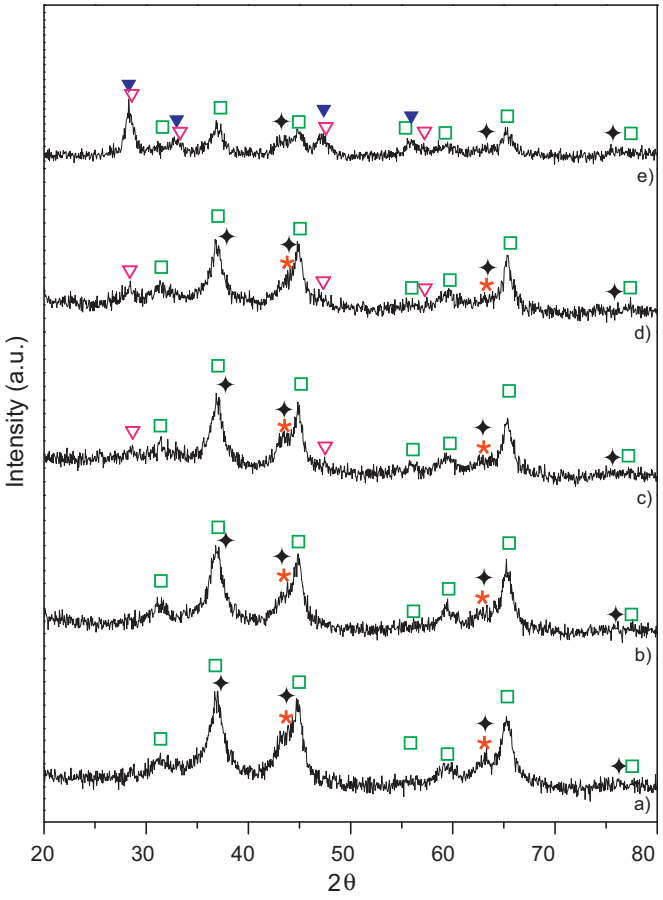

Fig. 1. Diffraction patterns of fresh catalysts: (a) $Ni/Pr_0/MgAl$, (b) $Ni/Pr_1/MgAl$, (c) $Ni/Pr_3/MgAl$, (d) $Ni/Pr_5/MgAl$ and (e) $Ni/Pr_{10}/MgAl$. □: $MgAl_2O_4$, ★: MgO, ✦: NiO, ▽: PrO_2, and ▼: Pr_6O_{11}.

praseodymium composition determined by ICP is also shown in Table 1. Important differences with nominal values were observed due to the Pr source which was highly hygroscopic.

The diffraction patterns for fresh samples are illustrated in Fig. 1. In all the cases broad diffraction peaks corresponding to $MgAl_2O_4$ (2θ = 19.03°, 31.3°, 36.8°, 44,8°, 55.6°, 59.4° and 65.2°, JCPDS-21-1152) and NiO (2θ = 43.3°, 37.3°,62.9°, JCPDS-4-835) were detected. The broadening lines of aluminate phase indicated that higher temperatures are required to reach a high crystallinity. This has been reported in literature for other synthesis methods [36,40–42]. Besides, peaks which intensities increased with Pr loading corresponding to PrO_2 (2θ = 28.7°, 33.2.°, 47.7°, 56.6°, JCPDS-24-1006) were also observed in the samples with Pr. The peak intensities were weak except for $Ni/Pr_{10}/MgAl$. The presence of Pr_6O_{11} considered as an oxygen-deficient modification of PrO_2 could not be ruled out since many reflection lines are nearly coincident (2θ = 28.2°, 47°, 32.7°, 55.7°, JCPDS-42-1121). Gallego et al. have reported the presence of both oxides, PrO_2 and Pr_6O_{11} over $PrNiO_3$ catalysts calcined at 700 °C [33]. The formation of MgO could not be ruled out since the most intense reflection lines (2θ = 36.9°, 42.9°, 62.3°, JCPDS-4-829) are nearly coincident with NiO, even if it was present, its amount would be small due to its consumption in the spinel formation.

Temperature programmed reduction measurement profiles are presented in Fig. 2 (a–e). The TPR for $Ni/Pr_0/MgAl$ showed hydrogen consumption between 450 and 700 °C, with a maximum at ≈680 °C. This peak corresponds to the Ni^{+2} species of NiO which are strongly interacted in aluminate matrix. This TPR profile was similar to others in literature [36,43,44]. A reduction peak between

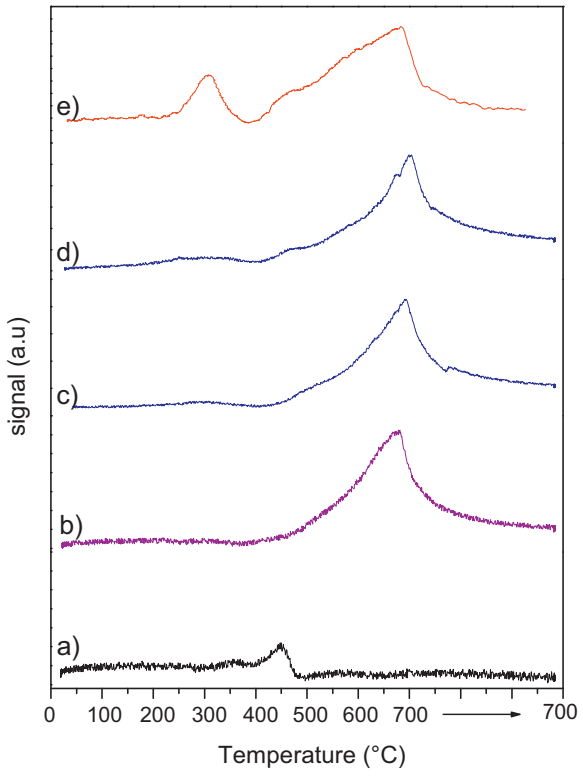

Fig. 2. Temperature programmed reduction of (a) Pr_5/MgAl, (b) Ni/Pr_0/MgAl, (c) Ni/Pr_1/MgAl, (d) Ni/Pr_5/MgAl and (e) Ni/Pr_{10}/MgAl catalysts.

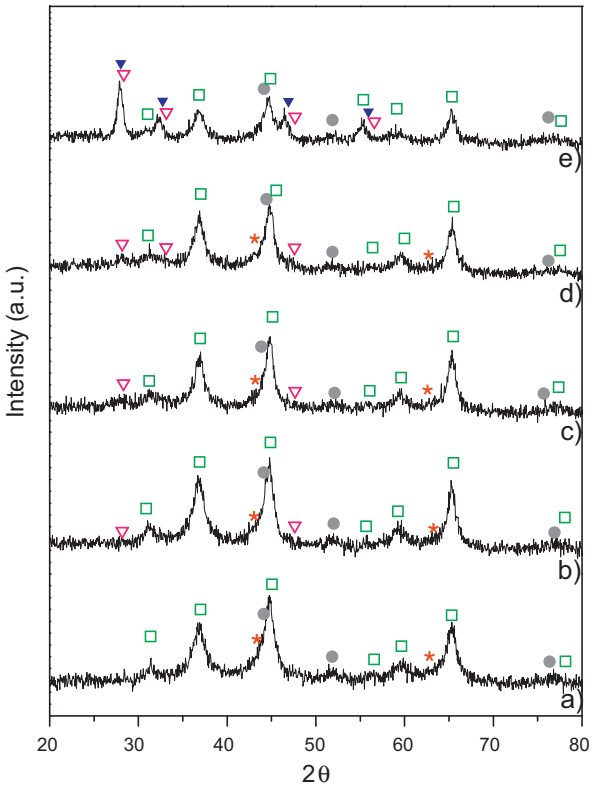

Fig. 3. Diffraction patterns of reduced catalysts: (a) Ni/Pr_0/MgAl, (b) Ni/Pr_1/MgAl, (c) Ni/Pr_3/MgAl, (d) Ni/Pr_5/MgAl and (e) Ni/Pr_{10}/MgAl. □ : $MgAl_2O_4$, ★ : MgO, ●: Ni, ▽ : PrO_2, and ▼ : Pr_6O_{11}.

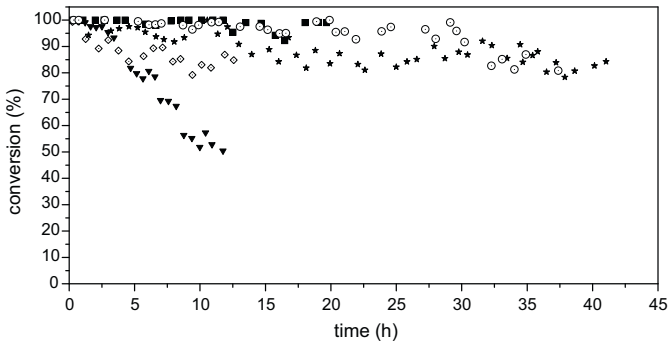

Fig. 4. Ethanol conversion over Ni/Pr_x/MgAl catalysts as a function of time. ▼: Ni/Pr_0/MgAl, ◊: Ni/Pr_1/MgAl, ■: Ni/Pr_3/MgAl, ⋆: Ni/Pr_5/MgAl, and ○: Ni/Pr_{10}/MgAl.

380 and 830 °C attributed to Ni^{+2} strongly interacted with the aluminate was reported for Ni/MgO–Al_2O_3 catalyst calcined at 650 °C [43]. Corthals et al. have also described one peak in the temperature range of 700–1000 °C for catalysts with Ni(10 wt.%)/$MgAl_2O_4$ [44]. TPR profiles for Pr samples are similar. They presented an intense peak around 700 °C which again suggests the presence of Ni^{2+} species with a strong extent of interaction metal-support; a shoulder around 480 °C, which could be assigned to the surface praseodymium oxide reduction and/or probably to a contribution of Ni^{2+} species from NiO with lower interaction; and a first peak around 300 °C which intensity increases with Pr loading attributed to the surface praseodymium oxide reduction. A TPR experiment for a Ni free sample with Pr (nominal wt.%5) supported on $MgAl_2O_4$ was carried out and the profile is also shown in Fig. 2. Two weak peaks were observed at 354 and 451 °C. Praseodymium oxides have similar properties of ceria [29] and it is well known that the reduction of surface oxygen in CeO_2 is promoted by the presence of metal [45]. Then it could be plausible that the presence of nickel promotes the surface PrO_2/ Pr_6O_{11} reduction. In all samples, the reduction led to metallic nickel as determined by XRD. In Fig. 3 (a–d), diffraction patterns of reduced samples after TPR experiments are shown. They revealed the absence of NiO peaks and the presence of lines corresponding to Ni^0 ($2\theta = 44.5°$, 51.8°, JCPDS-4-0850) related to the crystalline plane (1 1 0) and (2 0 0). No significant changes were observed in the remaining phases.

In almost all the cases reported in literature the catalysts are reduced in hydrogen before reforming reaction. This previous treatment at high temperatures could lead sintering of Ni particles and consequently increase the tendency to carbon formation. The elimination of this step would have a positive effect besides, it could simplify the operation of a reformer-purificator-fuel cell assembly. In this work the catalytic activity was studied over all catalysts at 650 °C without a previous reduction. The ethanol conversion as a function of time is shown in Fig. 4. Although, a high activity was observed for Ni/Pr_0/MgAl the sample was quickly deactivated with time on stream. Ethanol conversion decreased from 100% to 50.5% after 700 min. After this reaction time the experimental run was interrupted due to catalyst bed plugging. A lower loss activity was observed for 0.6 wt.% of Pr sample. The conversion decreased from 100% to 85% after 100 min and then it remained nearly constant until 750 min. The pressure in the catalyst bed was increased after this operation time and the experimental run had to be interrupted. The addition of 1.8 wt.% Pr markedly improved the conversion (100% during 1200 min) but again the run had to be interrupted after this time by building up of pressure. Under the experimental conditions used, which are more severe than those often reported in literature, a high carbon deposition rate would be responsible for this behavior (shown further).

The addition of 2.6 or 6.7 wt.% Pr slowed down the rate of deactivation since the ethanol conversion was maintained nearly constant more than 2000 min. However, the pressure in the cat-

alysts bed increased after 2250 min on $Ni/Pr_{10}/MgAl$ catalyst. On the contrary, the catalyst with 2.6 wt.% Pr could work for around 2500 min without changes of pressure in the reactor. At this TOS the run was precisely interrupted. These results suggest an optimum amount of Pr and deserve further studies. Probably, the major amount of Pr_6O_{11} on $Ni/Pr_{10}/MgAl$ could adversely affect the catalytic behavior.

In Fig. 5 the product distribution for all catalysts is shown. At 650 °C the main products were H_2, CO_2, CO, CH_4 and C_2H_4O. For $Ni/Pr_0/MgAl$ a significant amount of C_2H_4O was detected increasing with time on stream at expense of CO_2 and H_2. The CO and CH_4 selectivities were nearly constant around 30 and 10%, respectively. The H_2 yield decreased from 4.8 to 3 mol H_2/mol C_2H_5OH. Other products such as ethene, acetone and propane were also obtained with selectivities lower than 2%. For Pr catalysts the product distribution was nearly stable during the time on stream. The H_2 selectivity was around 4.5–5 mol H_2/mol C_2H_5OH. Except to $Ni/Pr_{10}/MgAl$, the CO/CO_2 molar ratio was higher than that observed on the Pr free catalyst. It is well known that the presence of CO in the observed reaction products is a consequence of different reactions involving ethanol and water, such as ethanol decomposition ($C_2H_5OH \rightarrow H_2 + CO + CH_4$). An increase in CO formation on these catalysts with Pr could be related to a contribution of carbon removal reactions such as Boudouard reaction, according to the stoichiometric equation: $CO_2 + C_{(A)} = 2\ CO$, being $C_{(A)}$ amorphous carbon ($\Delta G^0_{600\,^\circ C} = -4.4\ kJ\ mol^{-1}$) [24] which could be favored by the presence of praseodymium oxides. In the dry reforming of methane over $La_{1-x}Pr_xNiO_{3-d}$ perovskites, Gallego et al. [33] have related the decreasing amount of carbon deposit to the redox properties of praseodymium oxides and they have suggested the following reactions:

$$Pr_2O_3 + CO_2 \rightarrow 2PrO_2 + CO$$

$$4PrO_2 + C \rightarrow 2Pr_2O_3 + CO_2$$

In order to explain the differences in catalytic stability and clarify the effect of Pr addition, the post reaction characterization was carried out.

XRD of spent catalyst are shown in Fig. 6. The diffraction patterns illustrated in Fig. 6 (a–d) revealed the corresponding peaks of $MgAl_2O_4$ indicating that the support structure was maintained during reaction. The typical reflection of Ni^0 (2 0 0) was also clearly shown due to the Ni^{2+} reduction under reforming conditions. Weak reflections assigned to NiO or MgO were also detected. Although an incipient peak at $2\theta = 28.2–28.3^\circ$ was detected, there were not praseodymium phases clearly visible in the diffractograms. This peak could be an indication of the some oxygen-deficient praseodymium oxides presence. For the sample with the highest Pr loading the intensities of the peaks have almost disappeared due to the great carbon amount formed during reaction which extinguishes the X-ray, Fig. 6(e). In all XRD patterns an additional broad peak corresponding to graphite at $2\theta = 26.4^\circ$ (JCPDS-41-1487) was observed. Its intensity decreases from 0 to 2.6 wt.% Pr in agreement with carbon amount determined by TPO (see further). Corthals et al. have also reported the formation of this type of carbon on Ni(10 wt.%)/$MgAl_2O_4$ (modified with CeO_2 and ZrO_2) in the dry reforming of methane [44].

The nature and characteristics of carbon deposits were studied by Raman spectroscopy and temperature programmed oxidation experiments. In all the cases the Raman spectra of spent samples (not shown) in the range of 1000–1700 cm^{-1} revealed two broad bands centered at 1581 cm^{-1} and 1343 cm^{-1} which indicates the presence of ordered carbon, graphitic type, and disordered defective structures, respectively. The band at 1343 cm^{-1}, known as D band, was more intense than the band at 1581 cm^{-1}, known as

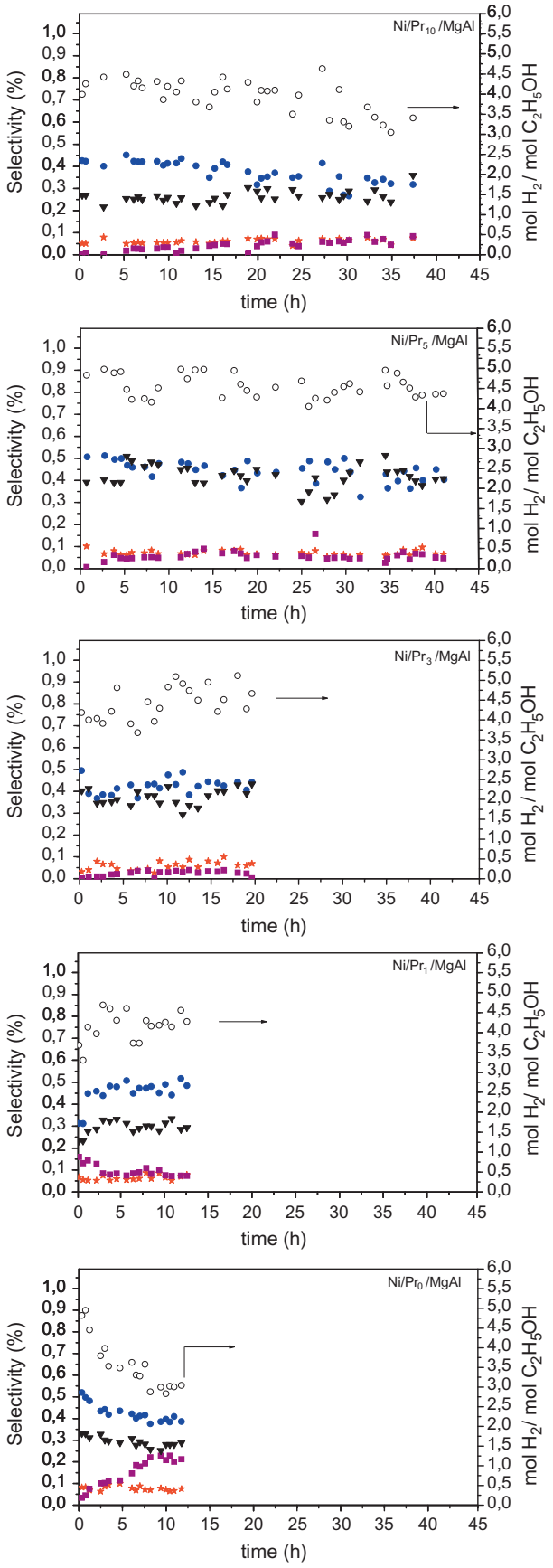

Fig. 5. Product distribution in the ethanol steam reforming over $Ni/Pr_x/MgAl$ catalysts. ○: mol H_2/mol C_2H_5OH, ■: C_2H_4O, ★: CH_4, ●: CO_2, and ▼: CO.

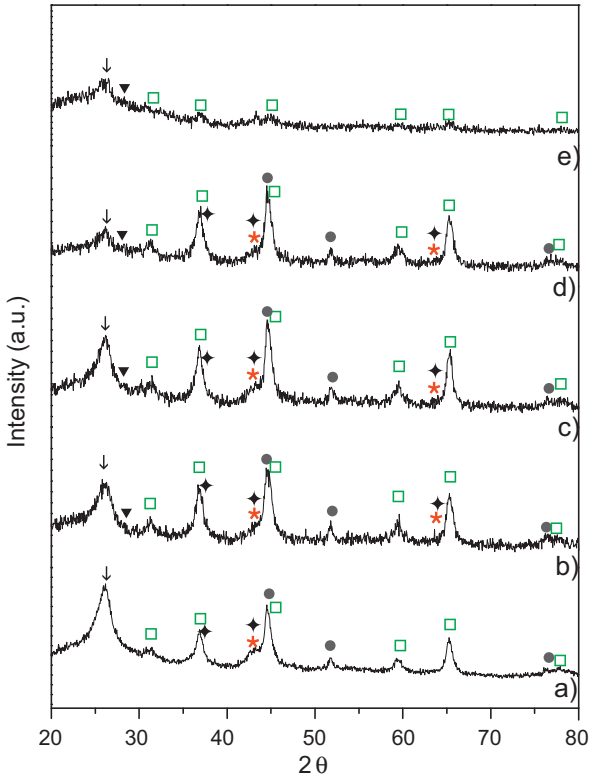

Fig. 6. Diffraction patterns of spent catalysts: (a) $Ni/Pr_0/MgAl$, (b) $Ni/Pr_1/MgAl$, (c) $Ni/Pr_3/MgAl$, (d) $Ni/Pr_5/MgAl$ and (e) $Ni/Pr_{10}/MgAl$. □: $MgAl_2O_4$, ●: Ni, ✦: NiO, ★ MgO, ↓ C, and ▼: PrO_{2-x}.

G band. Then, a predominance of disordered structures such as amorphous carbon, nanoparticles of carbon or filamentous can be concluded [46]. In spite of having no differences in the carbon structures with the Pr addition, differences in the relative intensity of the bands were observed. The D band intensity was always higher than G band. From Table 2, it is observed that the I_G and I_D values are substantially lower on $Ni/Pr_5/MgAl$ (it should be taken into account that samples were used at different TOS) in agreement with the higher stability observed.

The amount of carbon deposited on each catalyst was determined by temperature programmed oxidation by means of thermogravimetry. The results are shown in Table 2. In all the cases the oxidation of carbon deposits occurred between 500 and 700 °C in agreement with data in literature [36,47]. In all samples, two kinds of carbon with differences in their abundances were determined by Raman. The amounts of each type depended on the TOS and the Pr loading. The addition of 2.6 and 6.7 wt.% Pr shifted the combustion temperature at higher values which could be an indication that the carbon graphitic fraction on these samples was more graphitic and less reactive [43]. This carbon should be deposited on aluminate matrix and as filaments on metallic particles. After 700 °C all samples reached a constant weight indicating that all carbon was removed by oxidation. The total amount of carbon expressed as mmol of carbon per mol of reacted ethanol, Table 2, was similar for 0, 0.6, 1.8 wt.% Pr. However, the carbon amount for $Ni/Pr_5/MgAl$ was substantially lower taking into account that the TOS was three times higher. These results agree with those of XRD. A large amount of carbon was determined on $Ni/Pr_{10}/MgAl$ although the catalytic activity could be kept for 2250 min. This suggests that an important fraction of this carbon was deposited in multilayers with loose structure over support surface and does not hamper the reactant gases diffusion to the catalyst. Besides, a fraction of Ni was accessible to the reactant gases during this time. Finally, the carbon amount is enough for plugging the reactor.

The formation of carbon deposit on the spent catalyst was also evidenced by SEM observations. In Fig. 7, the micrographs of $Ni/Pr_0/MgAl$ and $Ni/Pr_5/MgAl$ fresh and spent catalysts are presented. The SEM micrographs for fresh samples are similar with domains of different morphology, Fig. 7A (a) and B (a). EDS analysis in different zones showed areas rich in praseodymium and nickel which allows to assume that they were not homogeneously distributed. For spent $Ni/Pr_0/MgAl$ sample the presence of filaments was not observed under the detection limits of technique, Fig. 7A (b). Since carbon deposits were revealed by XRD and TPO-TG, it can be inferred that an amorphous type of carbon mainly covers the support and encapsulates the metallic particles. This explains the quick deactivation of this catalyst (from 100% to 50%). The Ni signal in the EDS analysis for this sample has almost disappeared due to the important carbon coverage. A significant change in morphology was observed in SEM micrograph of $Ni/Pr_5/MgAl$ spent catalyst, Fig. 7B (b). In addition to amorphous carbon, a well defined fibrous conformation clearly appeared. The deactivation was not so severe as for $Ni/Pr_0/MgAl$, then it could be suggested that an important Ni^0 fraction continued exposed at the reactive mixture in the top of filaments and the carbon species which were not in contact with metallic particles were partially removed by gasification or Boudouard reaction. Filaments were observed by SEM in all Pr samples (not shown), then the presence of Pr modified the carbon deposition mechanism.

Recently, Coleman et al. have studied the ethanol steam reforming reaction over Ni catalysts supported on aluminium–magnesium mixed oxides with molar ratio Mg:Al = 2:1 and 1:2 [48]. Under similar operation conditions except for water concentration, these catalysts showed no deactivation for 20 h at 650 °C. The authors did not inform about changes in pressure of catalyst bed during this period although the carbon amount was substantially higher than that observed on $Ni/Pr_5/MgAl$ (0.048 > 0.013 mg C/g C_2H_5OH converted). The molar ratio H_2O:C_2H_5OH was 8.4 being almost the double than the molar ratio used in this work (4.9). It is well known the influence of water in the deactivation of reforming catalysts. Resini et al. [49] have also studied Ni–Mg–Al catalysts. Their results were presented as ethanol conversion (100% at 650 °C) and product

Table 2
Carbon amounts and Raman results of spent catalysts.

Catalyst	TOS (min)	T_{TPO} (°C)	mmol C/mol C_2H_5OH[a]	Raman		
				I_G	I_D	I_G/I_D
$Ni/Pr_0/MgAl$	700	639	0.23	7.82	12.3	0.64
$Ni/Pr_1/MgAl$	750	630	0.28	18.51	23.38	0.78
$Ni/Pr_3/MgAl$	1180	610	0.22	26.88	34.57	0.77
$Ni/Pr_5/MgAl$	2460	653	0.05	3.21	5.66	0.57
$Ni/Pr_{10}/MgAl$	2250	688	1.12	11.52	16.85	0.68

TOS: time on stream.
[a] Determined from C amount/ (F^{in}_{EtOH} TOS $X_{average}$).

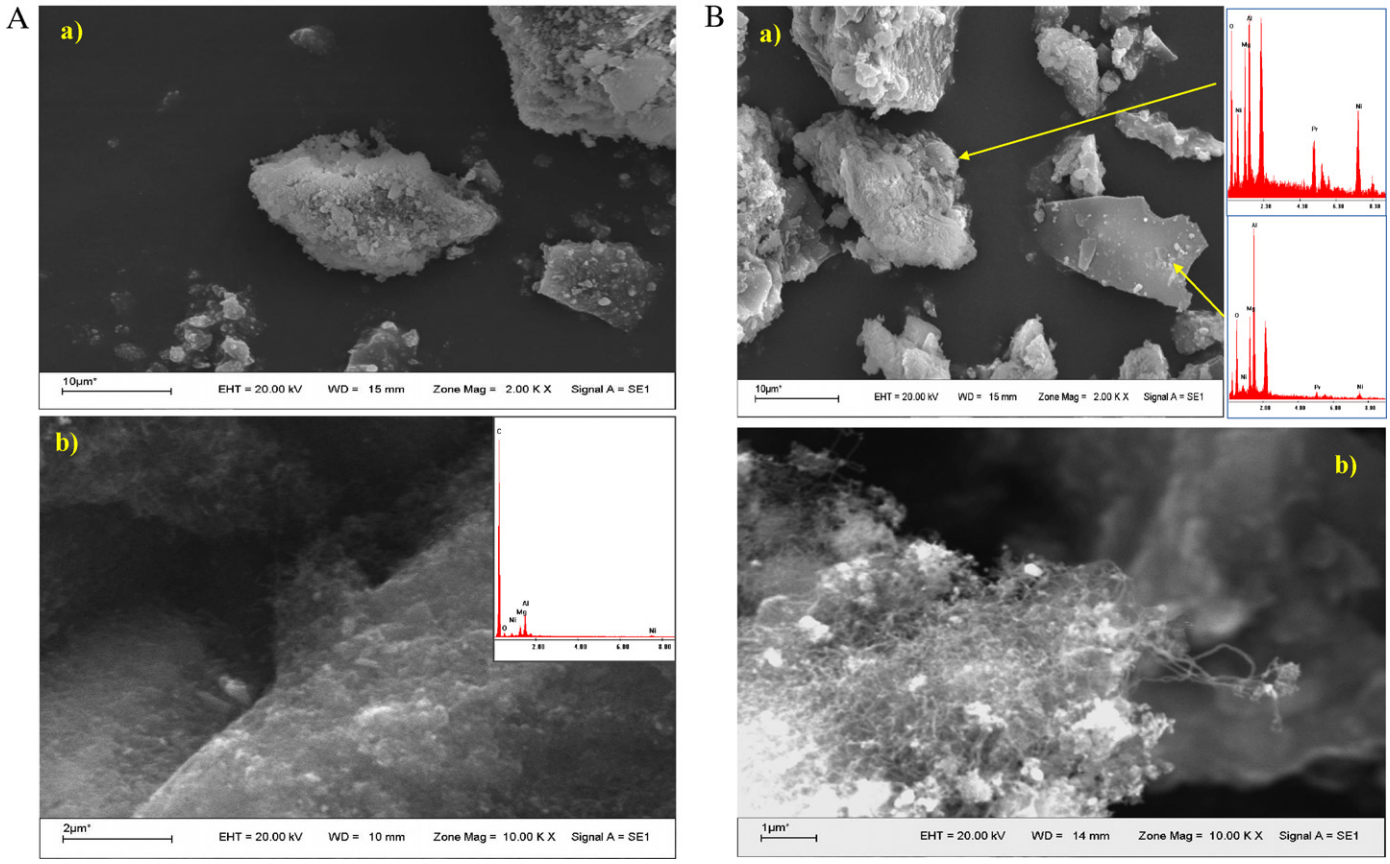

Fig. 7. SEM micrographs and EDX spectra of (a) fresh catalysts and (b) after ethanol steam reforming at 650 °C. (A) Ni/Pr_0/MgAl and (B) Ni/Pr_5/MgAl.

distribution against reaction temperature however, the authors did not report stability tests.

4. Conclusions

Ni catalysts supported on a modified magnesium aluminate were prepared and evaluated in ethanol steam reforming. The Ni loading (8 wt.%) was constant and the amount of Pr varied from 0 to 7 wt.%. The Pr presence did not substantially change the textural and morphologic properties. The Ni^{2+} reducibility was not substantially modified by Pr addition but the ability of praseodymium oxides to suffer redox process under reaction conditions was an important characteristic of Pr samples. The Pr addition slowed down the rate of deactivation affecting the amount and the type of carbon deposits.

The catalyst with 2.6 wt.% Pr showed a high activity at 650 °C (around 80%) and stability, but fibrous carbon was formed during reaction. The highest resistance to deactivation was ascribed to the redox properties of praseodymium oxides.

Acknowledgments

Financial supports are acknowledged to CONICET, ANPCyT and Universidad Nacional de San Luis. The authors wish to thank Dr. John Múnera and Dr. Raul Gil for Raman and ICP assistances, Dr. Luis Arrúa for helpful discussions and M. Gomez for participating in experimental work. Furthermore, we are very grateful to Dr. Julio Andrade Gamboa for valuable discussions in XRD results. The funds from the ANPCyT to buy the Raman instrument are also gratefully acknowledged (PME 87-PAE 36985).

References

[1] P.G. Gray, M.I. Petch, Platinum Met. Rev. 44 (2000) 108.
[2] N. Edwars, S.R. Ellis, J.C. Frost, S.E. Golunski, A.N.J. van Keulen, N.G. Lindewald, J.G. Reinkingh, J. Power Sources 71 (1998) 123.
[3] M. Laborde, Producción y Purificación de hidrógeno a partir de bioetanol y su aplicación en pilas de combustibles, CYTED, Buenos Aires, 2006, ISBN 987-05-1795-1, ISBN-13: 978-987-05-1795-1.
[4] J.C. Vargas, S. Libs, A.C. Roger, A.C. Kiennemann, Catal. Today 417 (2005) 107.
[5] J.P. Breen, R. Burch, H.M. Coleman, Appl. Catal. B 39 (2002) 65.
[6] V.V. Galvita, G.L. Semin, V.D. Belyaev, V.A. Semikolenov, P. Tsiakaras, V.A. Sobyanin, Appl. Catal. A 220 (2001) 123.
[7] F. Auprêtre, C. Descorme, D. Duprez, Catal. Commun. 3 (2002) 267.
[8] D.K. Liguras, I. Kondarides, X.E. Verykios, Appl. Catal. B 43 (2003) 345.
[9] A.N. Fatsikostas, D.I. Kondarides, X.E. Verykios, Catal. Today 75 (2002) 145.
[10] S. Freni, S. Cavallaro, N. Mondello, L. Spadaro, F. Frusteri, Catal. Commun. 4 (2003) 259.
[11] M.N. Barroso, M.F. Gomez, L.A. Arrúa, M.C. Abello, Appl. Catal. A 304 (2006) 116.
[12] F. Mariño, G. Baronetti, M. Jobbagy, M. Laborde, Appl. Catal. A 238 (2003) 41.
[13] V. Klouz, V. Fierro, P. Denton, H. Katz, J.P. Lisse, S. Bouvot-Mauduit, C. Mirodatos, J. Power Sources 105 (2002) 26.
[14] F. Haga, T. Nakajima, H. Miya, S. Mishima, Catal. Lett. 48 (1997) 223.
[15] J. Llorca, N. Homs, J. Sales, P. Ramírez de la Piscina, J. Catal. 209 (2002) 306.
[16] J. Llorca, J.A. Dalmon, P. Ramírez de la Piscina, N. Homs, Appl. Catal. A 243 (2003) 261.
[17] J. Llorca, P. Ramírez de la Piscina, J.A. Dalmon, J. Sales, N. Homs, Appl. Catal. B 43 (2003) 355.
[18] M.C. Batista, R.K.S. Santos, E.M. Assaf, J.M. Assaf, E.A. Ticianelli, J. Power Sources 124 (2003) 99.
[19] D.R. Sahoo, S. Vajpai, S. Patel, K.K. Pant, Chem. Eng. J. 125 (2007) 139.
[20] H. Song, L.Z. Zhang, U. Ozkan, Catal. Today 129 (2007) 346.
[21] S.-Y. Lin, D.H. Kim, S.Y. Ha, Appl. Catal. A 355 (2009) 69.
[22] H. Song, U. Ozkan, J. Catal. 261 (2009) 66.
[23] J. Sehested, Catal. Today 111 (2006) 103.
[24] A. Galetti, M. Gomez, L. Arrúa, A. Marchi, M.C. Abello, Catal. Commun. 9 (2008) 1201.
[25] A. Galetti, M. Gomez, L. Arrúa, M.C. Abello, Appl. Catal. A 348 (2008) 94.
[26] A. Vizcaíno, P. Arena, G. Baronetti, A. Carrero, J. Calles, M. Laborde, N. Amadeo, Int. J. Hydrogen Energy 33 (2008) 3489.
[27] A.L. Alberton, M.M.V.M. Souza, M. Schmal, Catal. Today 123 (2007) 257.

[28] A. Galetti, M. Gomez, L. Arrúa, M.C. Abello, Appl. Catal. A 380 (1–2) (2010) 40.
[29] D.R. Mullins, Surf. Sci. 556 (2004) 159.
[30] V. Thangadurai, R.A. Huggins, W. Weppnar, J. Solid State Electrochem. 5 (2001) 531.
[31] D.R. Mullins, K. Zhang, J. Phys. Chem. B 105 (2001) 1374.
[32] Y. Borchert, P. Sonström, M. Wilhelm, H. Borchert, M. Bäumer, J. Phys. Chem. C 112 (2008) 3054.
[33] G. Gallego, J. Marin, C. Batiot-Dupeyrat, J. Barrault, F. Mondragón, Appl. Catal. A 369 (2009) 97.
[34] J. Sehested, J.A.P. Gelten, I.N. Remediakis, H. Bengaard, J.K. Norskov, J. Catal. 223 (2004) 432.
[35] A.M. Gadalla, B. Bower, Chem. Eng. Sci. 43 (1988) 3094.
[36] J. Guo, H. Lou, H. Zhao, D. Chai, X. Zheng, Appl. Catal. A 273 (2004) 75.
[37] F. Auprêtre, C. Descorme, D. Duprez, D. Casanave, D. Uzio, J. Catal. 233 (2005) 464.
[38] M.N. Barroso, M.F. Gomez, L.A. Arrua, M.C. Abello, Actas XVI CAC, Buenos Aires, 2009.
[39] P. Malet, A. Caballero, J. Chem. Soc. Faraday Trans. 84 (1988) 2369.
[40] J. Guo, H. Lou, H. Zhao, X. Wang, X. Zheng, Mater. Lett. 58 (2004) 1920.
[41] E.L. Foletto, R.W. Alves, S.L. Jahn, J. Power Sources 161 (2006) 531.
[42] H. Zhang, X. Jia, Z. Liu, Z. Li, Mater. Lett. 58 (2004) 1625.
[43] M. Sánchez-Sánchez, R.M. Navarro, J.L.G. Fierro, Int. J. Hydrogen Energy 32 (2007) 1462.
[44] S. Corthals, J. Van Nederkassel, J. Geboers, H. De Winne, J. Van Noyen, B. Moens, B. Sels, P. Jacobs, Catal. Today 138 (2008) 28.
[45] X. Tang, B. Zhang, Y. Li, Y. Xu, Q. Xin, W. Shen, Appl. Catal. A 288 (2005) 116.
[46] F. Pompeo, N. Nichio, O. Ferretti, D. Resasco, Int. J. Hydrogen Energy 30 (2005) 1399.
[47] A. Nadini, K. Pant, S. Dhingra, Appl. Catal. A 290 (2005) 166.
[48] L.J.I. Coleman, W. Epling, R.R. Hudgins, E. Croiset, Appl. Catal. A 363 (2009) 52.
[49] C. Resini, T. Montanari, L. Barattini, G. Ramis, G. Busca, S. Presto, P. Riani, R. Marazza, M. Sisani, F. Marmottini, U. Costantino, Appl. Catal. A 355 (2009) 83.